

Brain Perfusion SPECT with ^{99m}Tc -Bicisate: Comparison with PET Measurement and Linearization Based on Permeability-Surface Area Product Model

Yoshiharu Yonekura, *Tatsuro Tsuchida, *Norihiro Sadato, *Sadahiko Nishizawa, *Yasushi Iwasaki, *Takao Mukai, *Junji Konishi, and Hiroshi Shibasaki

Departments of Brain Pathophysiology and *Nuclear Medicine, Kyoto University School of Medicine, Kyoto, Japan

Summary: To characterize a recently introduced cerebral perfusion tracer, ^{99m}Tc -bicisate, single photon emission computed tomography (SPECT) images of ^{99m}Tc -bicisate were compared with CBF images obtained by positron emission tomography (PET) using the ^{15}O steady-state method in 10 cases of cerebrovascular disease and dementia. ^{99m}Tc -Bicisate SPECT and PET CBF images showed a similar distribution pattern except for two cases with subacute stroke, in which ^{99m}Tc -bicisate showed less uptake than CBF in the infarcted area where oxygen metabolism was severely diminished. Comparison of ^{99m}Tc -bicisate uptake and CBF in the other eight cases showed less contrast between high- and low-flow regions in ^{99m}Tc -bicisate SPECT. Although the SPECT count ra-

tio of cerebral structures to cerebellum showed a good correlation with CBF ratio, it gradually deviated from the linear relationship in the high-flow range. Assuming this nonlinear relationship is due to the limited extraction of the tracer, we estimated the permeability-surface area product (*PS*) value by a nonlinear least-squares curve-fitting procedure. The correction of the nonlinear relationship using the estimated *PS* value and a table lookup method resulted in an excellent linear relationship between corrected SPECT counts and CBF. **Key Words:** ^{99m}Tc -Bicisate—Brain perfusion—Cerebral blood flow—Positron emission tomography—Single photon emission computed tomography.

Over the last decade, rapid advancements in both instrumentation and radiopharmaceuticals have introduced an increasing interest in evaluation of regional CBF with the radionuclide approach. Although positron emission tomography (PET) still plays a major role in understanding the mechanism of normal brain function and the underlying pathophysiology of diseased brain function, the widespread availability of single photon emission computed tomography (SPECT) scanners and commercial delivery of new radiopharmaceuticals have made it possible to perform cerebral perfusion studies as routine nuclear medicine procedures.

Several radiolabeled tracers have been proposed for measurement of regional CBF (Winchell et al., 1980a; Kung et al., 1990), and some of them have been approved for clinical use. These tracers are classified into two groups: chemically inert tracers freely diffusing across the blood-brain barrier and trapping-type tracers that are retained by the brain, similar to microspheres. The former tracers have an advantage of quantitative capability for measurement in absolute flow values (Lassen, 1985), but require fast dynamic sampling and may not be suitable for SPECT imaging (Stokely et al., 1980). The latter tracers, on the other hand, can provide an excellent spatial resolution because of the longer acquisition time possible (Kuhl et al., 1982). The trapping mechanism of each tracer is different from that of others, and the kinetic behavior has to be understood well for the clinical application and interpretation of the SPECT images (Winchell et al., 1980b; Neirinckx et al., 1987).

The recently developed ^{99m}Tc -bicisate [^{99m}Tc -*N,N'*-(1,2-ethylenediyl)bis-L-cysteine diethyl ester;

Received May 7, 1993; final revision received September 3, 1993; accepted September 8, 1993.

Address correspondence and reprint requests to Dr. Y. Yonekura at Department of Brain Pathophysiology, Kyoto University School of Medicine, 54 Shogoin Kawahara-cho, Sakyo-ku, Kyoto 606-01, Japan.

Abbreviations used: FWHM, full width at half-maximum; OEF, oxygen extraction fraction; PET, positron emission tomography; ROI, region of interest; SPECT, single photon emission computed tomography.

^{99m}Tc -ECD] is a diester of a neutral ^{99m}Tc - N_2S_2 complex (Kung et al., 1989; Walovitch et al., 1989). This compound is optically active, and only the L,L-isomer shows prolonged retention in the brain (Léveillé et al., 1989; Vallabhajosula et al., 1989). The brain retention mechanism of this compound is proposed as the specific hydrolysis of one of the ester groups to monoacid, resulting in the trapping of hydrophilic monoacids in the brain (Walovitch et al., 1991). Clinical SPECT studies demonstrated an excellent image quality with little background activity (Léveillé et al., 1992). To characterize ^{99m}Tc -bicisate as a cerebral perfusion tracer, we compared ^{99m}Tc -bicisate SPECT images with CBF images obtained by PET and the ^{15}O steady-state method. We also applied the permeability-surface area product (*PS*) model (Crone, 1963; Raichle et al., 1976) to explain the nonlinear relationship between ^{99m}Tc -bicisate uptake and CBF and developed a method to correct CBF images with ^{99m}Tc -bicisate SPECT by a linearization procedure.

MATERIALS AND METHODS

Data acquisition

The study consisted of 10 paired ^{99m}Tc -bicisate SPECT examinations and PET measurements of CBF and oxygen metabolism in cerebrovascular disease and dementia. The patients included seven men and three women, whose ages ranged from 38 to 70 years. Five of them had chronic cerebrovascular disease and two subacute stroke. The other three subjects had dementia including two Alzheimer types and one Binswanger type. All patients received both ^{99m}Tc -bicisate SPECT examination and PET measurement of CBF and oxygen metabolism using the ^{15}O -gas inhalation method. The interval between SPECT and PET examination was within 2 days in subacute stroke and within 1 week in other cases. All subjects gave informed consent before the study.

^{99m}Tc -Bicisate was prepared from the cold kit (Daiichi Radioisotope Lab., Japan) and [^{99m}Tc]pertechnetate (30 mCi) obtained from the molybdenum-technetium generator. Approximately 20 mCi of ^{99m}Tc -bicisate was administered intravenously to each subject.

Brain perfusion SPECT imaging was performed at 30 min after injection of ^{99m}Tc -bicisate using a ring-type multidetector SPECT scanner (SET-030W; Shimadzu Co., Kyoto, Japan). The scanner simultaneously acquires three tomographic slices at 30-mm intervals. The spatial resolution was 12 mm full width at half-maximum (FWHM) in center, and the axial resolution was 23.5 mm FWHM (Yonekura et al., 1989). Two successive SPECT scans of 10-min acquisition each were performed to obtain the six interpolated SPECT slices at 15-mm intervals.

PET study was performed using a whole-body PET scanner (PCT-3600W; Hitachi Medical Co., Tokyo, Japan), which provided 15 PET slices at 7-mm intervals (Sadato et al., 1993). The intrinsic spatial resolution was 4.6 mm FWHM in center, but actual PET images obtained in this study were reconstructed at a resolution of 9 mm FWHM. The axial resolution was 6.5 mm FWHM.

The field of view and the pixel size of the reconstructed images were 256 and 2 mm, respectively. Prior to all emission scans, a transmission scan was performed using a standard plate source of $^{68}\text{Ge}/^{68}\text{Ga}$ for the correction of photon attenuation. Cross-calibration of the PET images to the radioactivity was performed using a cylindrical phantom filled with ^{18}F solution.

The subject's head was immobilized with head holders, and a small catheter was placed in the brachial artery for blood sampling. ^{15}O -labeled carbon dioxide, carbon monoxide, and molecular oxygen produced by a small cyclotron (Cyprius 325; Sumitomo Heavy Industries, Tokyo, Japan) were administered to the subjects using a radioactive gas inhalation system (AZ-711; Anzai Sogyo Co., Osaka, Japan). To obtain quantitative images of cerebral blood volume, CBF, oxygen extraction fraction (OEF), and CMRO_2 , bolus inhalation of ^{15}O -labeled CO and continuous inhalation of [^{13}O]CO₂ and O₂ with intermittent arterial blood sampling was performed (Frackowiak et al., 1980; Lammertsma and Jones, 1983a,b).

Data analysis

In addition to the visual comparison of ^{99m}Tc -bicisate SPECT and PET CBF images, we compared SPECT counts and CBF values in the regions of interest (ROIs). The original 15-slice PET images were first interpolated to create a three-dimensional volumetric data set of CBF with voxel size of $3.5 \times 3.5 \times 3.5$ mm. From these volumetric PET data, we selected the slices that were closest to the corresponding SPECT slices. After adjusting the pixel size of PET and SPECT images, both images were superimposed on the computer screen for visual registration by shifting and rotation. Then identical ROIs were placed on cerebral cortices (17×17 mm) and cerebellar hemispheres (23×23 mm) in PET and SPECT images. In each subject, several ROIs were placed in the frontal, temporal, parietal, and occipital cortices in bilateral cerebral hemispheres. In cases of cerebrovascular diseases, the ROI in the cerebellar hemisphere was placed ipsilateral to the cerebral lesion to exclude the effect of crossed cerebellar diaschisis or hypoperfusion (Baron et al., 1980; Yamauchi et al., 1992). The ratio of the value in each cortical region to that in the cerebellum (*C/Cb*) was compared between SPECT images and PET CBF images (Yonekura et al., 1988).

We propose a new linearization procedure for correction of a nonlinear relationship between regional CBF and SPECT counts based on the *PS* model (Crone, 1963). Assuming no back-diffusion of the tracer, regional activity of ^{99m}Tc -bicisate in the brain region (*C*) can be expressed by the following simple equation:

$$C = F \cdot E \int_0^T C_a(t) dt \quad (1)$$

where *F* is CBF ($\text{ml } 100 \text{ ml}^{-1} \text{ min}^{-1}$), *E* is the first-pass extraction, and $C_a(t)$ denotes the arterial input function. Based on the assumption of the *PS* model, *E* can be expressed as a function of *F* and *PS*:

$$E = 1 - \exp\left(\frac{-PS}{F}\right) \quad (2)$$

As we can assume identical input function to various regions of the brain in the same subject, the SPECT count

ratio to the reference region (C/C_r) can be expressed as a function of flow ratio (F/F_r) and PS as follows:

$$\frac{C}{C_r} = \frac{F}{F_r} \cdot \frac{1 - \exp(-PS/F)}{1 - \exp(-PS/F_r)} \quad (3)$$

This equation can be simplified as

$$Y = \frac{X(1 - Z^{1/X})}{1 - Z} \quad (4)$$

where $X = F/F_r$, $Y = C/C_r$, and $Z = \exp(-PS/F_r)$.

We applied this equation to estimate the PS value of ^{99m}Tc -bicisate using CBF measured by PET and the ^{15}O steady-state method. Ideally one should solve this equation in each subject because reference blood flow (F_r) may vary among the subjects. However, the data set in a single subject is not sufficient for estimation of PS value due to the small number of data points and the limited flow range. Therefore, we attempted to estimate the PS value with the larger number of data points in multiple subjects using cerebellar blood flow, which may show less variation among the subjects than other regions, as reference flow (F_r) (Yonekura et al., 1988). Equation 4 was used to evaluate a single best-fit value of Z using a nonlinear least-squares fitting method from the total com-

posite pattern of (X, Y) pairs obtained by PET measurement of CBF and ^{99m}Tc -bicisate SPECT. Then the PS value was estimated from this Z value using the average F_r value of the subjects.

Correction of SPECT counts was performed by the table lookup method using the PS value estimated by this procedure. Based on Eq. 4 for each X value a Y value was calculated to create a lookup table. To simplify the correction procedure, we applied fourth-order polynomial curve fitting for calculation of X from a given Y :

$$X = f(Y) = \sum_{i=0}^4 k_i Y^i \quad (5)$$

which was used for the correction of SPECT counts.

RESULTS

Visual comparison

SPECT images of ^{99m}Tc -bicisate demonstrated a good agreement with PET CBF images except for two cases with subacute cerebral infarction. Figure 1 shows SPECT and PET CBF images in a case

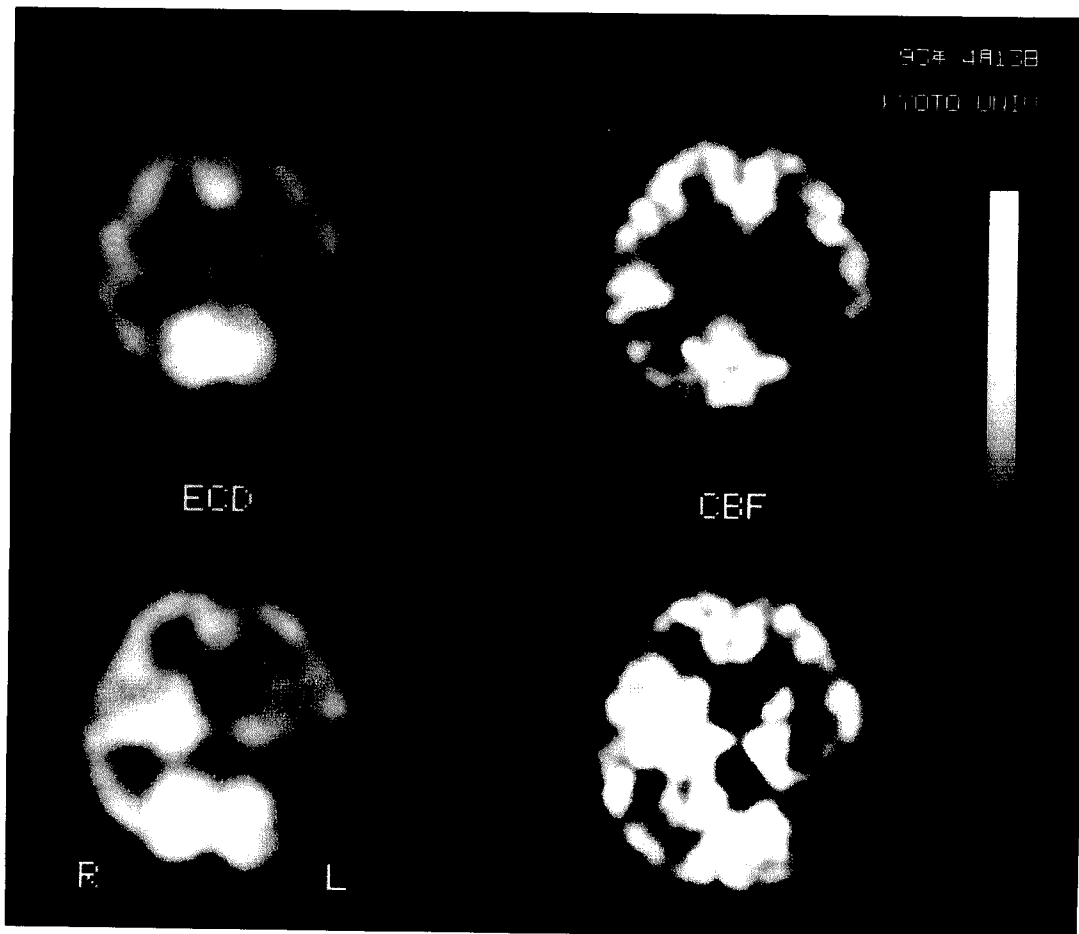


FIG. 1. ^{99m}Tc -Bicisate (ECD) single photon emission computed tomography (SPECT) and CBF positron emission tomography (PET) images in a case with chronic cerebral infarction. Both SPECT and PET showed a similar distribution pattern: decreased CBF in the left temporooccipital region.

with chronic cerebral infarction, demonstrating decreased CBF in the left temporooccipital region in both images. A similar relationship was also shown in dementia patients (Fig. 2).

In two cases of cerebral infarction examined in the subacute phase, ^{99m}Tc -bicisate SPECT showed decreased tracer accumulation in the infarcted area in spite of relatively preserved CBF measured by PET. Figure 3 shows ^{99m}Tc -bicisate SPECT and CBF PET images in one of these cases. The PET CBF image demonstrated well preserved perfusion in the right frontal region, while both OEF and CMRO_2 showed profound decreases, suggesting "luxury perfusion" in the infarcted lesion. In these cases, CMRO_2 in the infarcted area, which showed a defect by ^{99m}Tc -bicisate SPECT, was 0.73 and 0.68 ml O_2 $100 \text{ ml}^{-1} \text{ min}^{-1}$, indicating severe tissue damage.

Comparison of ^{99m}Tc -bicisate SPECT and PET CBF

Comparison of ^{99m}Tc -bicisate SPECT and CBF measured by PET in eight cases of chronic cerebro-

vascular disease and dementia demonstrated a good linear relationship in the low-flow range, which deviated from the linear relationship in the high-flow region. Figure 4 shows the comparison of the ^{99m}Tc -bicisate uptake ratio of the cerebral cortices to the cerebellum (C/C_r) and the result of nonlinear least-squares curve fitting, demonstrating a curvilinear relationship between ^{99m}Tc -bicisate uptake and CBF. The estimated Z value [$= \exp(-PS/Fr)$] was 0.243, and the average cerebellar blood flow (Fr) was $50.5 \text{ ml } 100 \text{ ml}^{-1} \text{ min}^{-1}$. The PS value calculated from these two parameters was $71 \text{ ml } 100 \text{ ml}^{-1} \text{ min}^{-1}$.

Correction of ^{99m}Tc -bicisate SPECT for linearization

Figure 5 demonstrates the effect of linearization correction for ^{99m}Tc -bicisate SPECT. The curvilinear relationship between the ^{99m}Tc -bicisate uptake ratio and the CBF ratio disappeared after the linearization procedure. The corrected ^{99m}Tc -bicisate

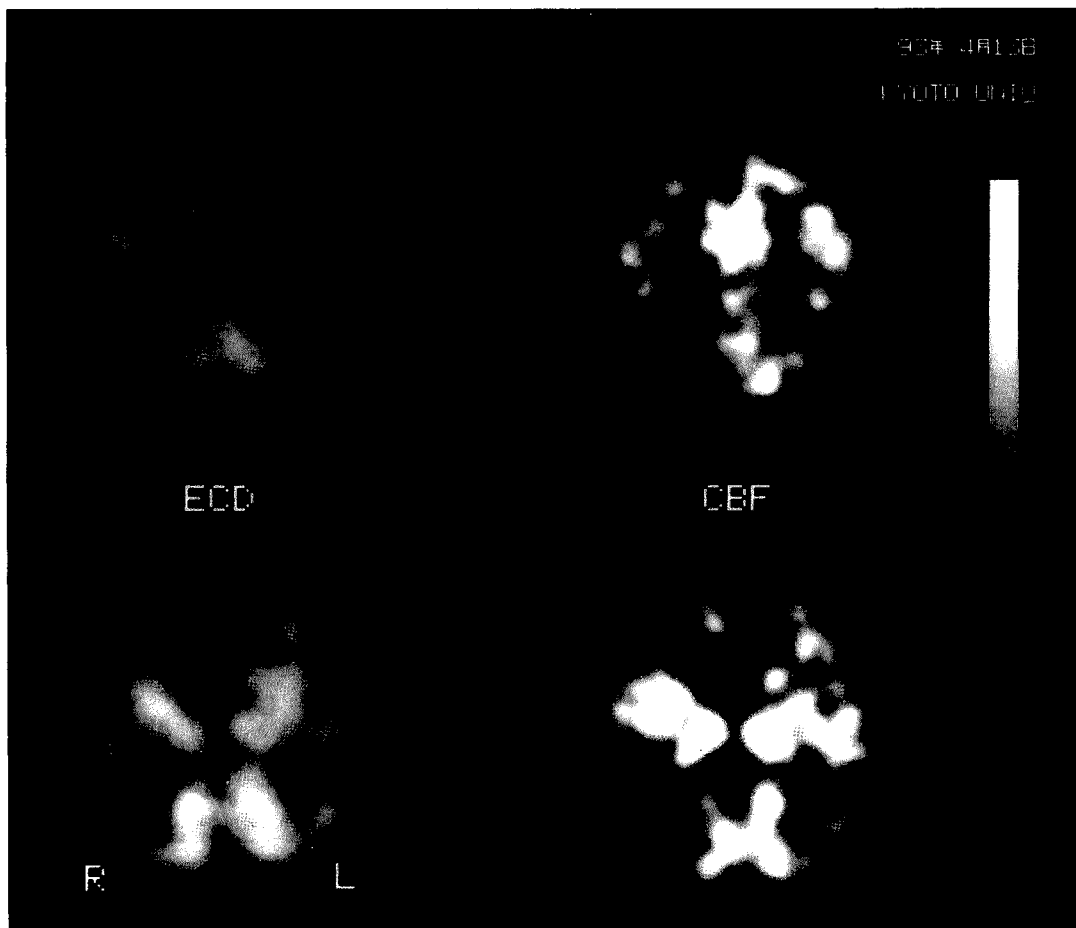


FIG. 2. ^{99m}Tc -Bicisate (ECD) single photon emission computed tomography (SPECT) and CBF positron emission tomography (PET) images in a case with dementia of the Alzheimer type. Both SPECT and PET showed decreased CBF in the bilateral left temporooccipital cortices.

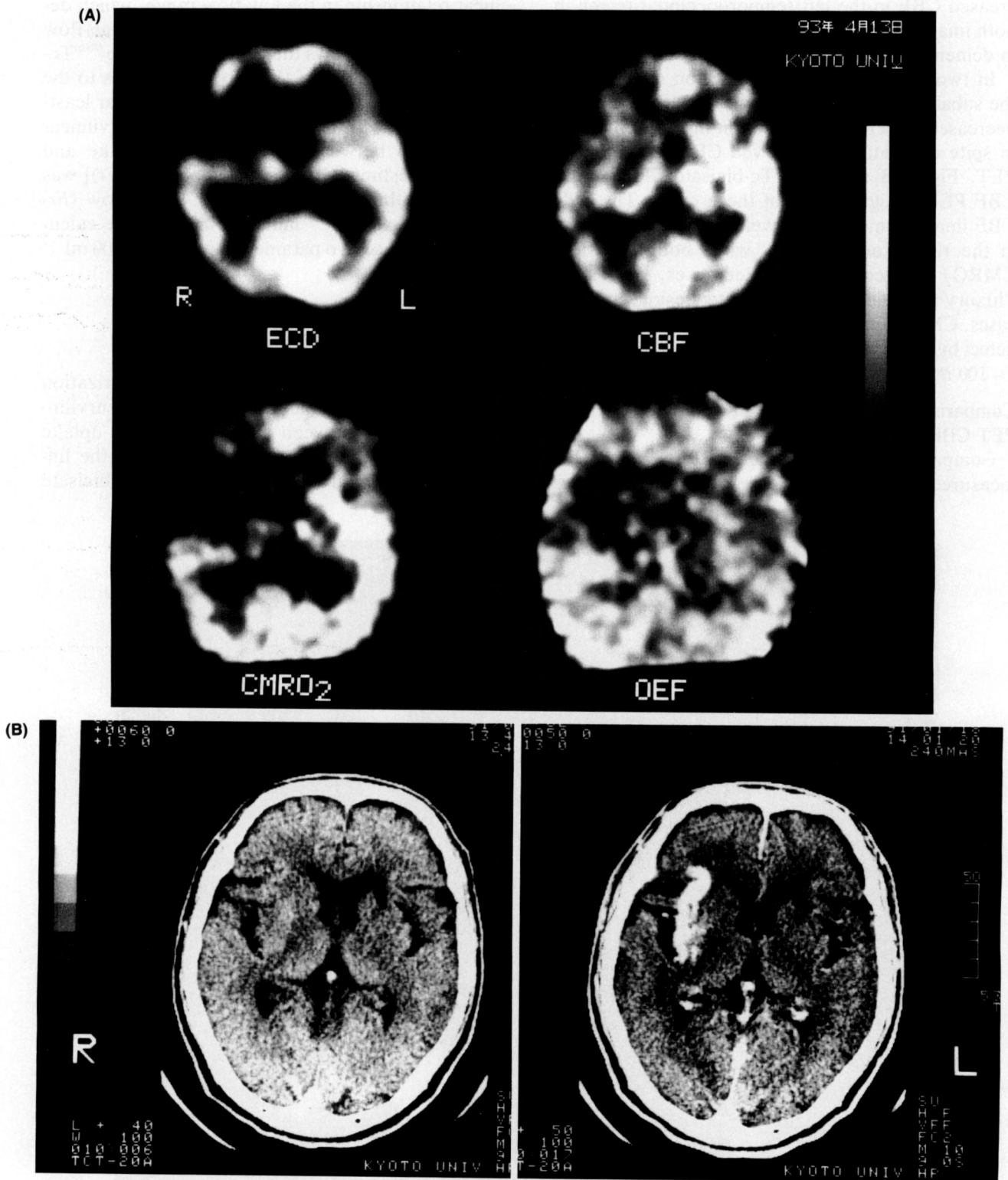


FIG. 3. Comparison of ^{99m}Tc -bicisate (ECD) single photon emission computed tomography (SPECT) and positron emission tomography (PET) CBF images in a case with subacute cerebral infarction (19 days after onset). ^{99m}Tc -Bicisate SPECT images showed decreased uptake in the right frontal region, corresponding to the infarction demonstrated by x-ray CT. PET on the same day demonstrated relatively preserved CBF with decreased oxygen extraction fraction (OEF) and CMRO_2 , suggesting relative luxury perfusion. **A:** ^{99m}Tc -Bicisate SPECT and PET images; **B:** x-ray CT images (left: plain CT; right: contrast-enhanced CT).

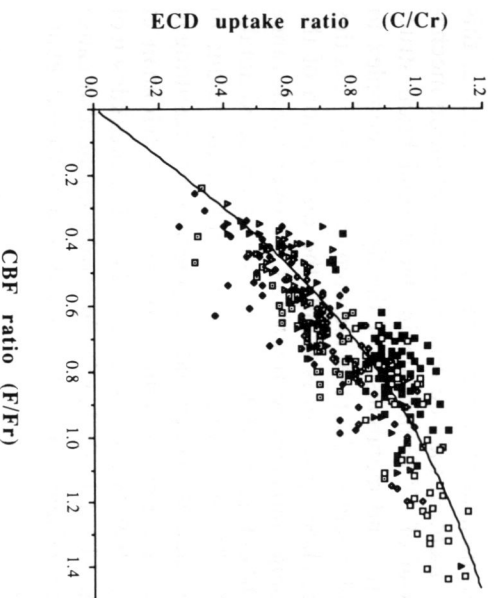


FIG. 4. Comparison of ^{99m}Tc -bicisate (ECD) uptake ratio and CBF ratio in eight cases, demonstrating curvilinear relationship in the high-flow range (F/Fr). The line represents the nonlinear curve-fitting analysis to estimate the Z value. Data sets of each subject were shown by different symbols.

uptake and CBF ratios demonstrated an excellent linear relationship ($y = 0.092 + 0.862x$, $r = 0.817$).

DISCUSSION

The present study demonstrated a similar distribution pattern of ^{99m}Tc -bicisate SPECT and PET CBF images in most cases except for subacute cerebral infarction, confirming the clinical feasibility of bicisate for evaluation of CBF. ^{99m}Tc -Bicisate SPECT showed less contrast between the decreased flow region and the normal CBF area. Although perhaps due partly to the different physical characteristics of PET and SPECT images, such as

spatial resolution, slice thickness, and scatter radiation, this could be explained by the kinetics of the tracer due to either the limited first-pass extraction of ^{99m}Tc -bicisate or back-diffusion of the tracer from the brain to the blood or both. Both limited extraction and back-diffusion decrease the SPECT counts, especially in the high-flow region, which is often seen with many flow tracers. Comparison of ^{99m}Tc -bicisate SPECT and PET CBF measurement demonstrated a nonlinear relationship between the tissue activity of ^{99m}Tc -bicisate and CBF.

^{99m}Tc -Bicisate was rapidly taken up and retained in the brain for a long time. The kinetics of bicisate were reported to be very similar both in humans and in nonhuman primates (Vallabhajosula et al., 1989). The first-pass extraction of ^{99m}Tc -bicisate was reported to be 77% in anesthetized monkey brain without apparent washout in the early phase (Walovich et al., 1989). In addition to the rapid blood clearance, ^{99m}Tc -bicisate shows rapid conversion from the original lipophilic compound to hydrophilic metabolites in brain and blood (Walovich et al., 1989). Therefore, the arterial input to brain is limited within the short period after intravenous injection. Based on these findings, we applied the PS model to explain the nonlinear relationship of ^{99m}Tc -bicisate uptake and CBF.

Obviously the estimation of the PS value by the present approach has several limitations, and the value of $71 \text{ ml } 100 \text{ ml}^{-1} \text{ min}^{-1}$ obtained in this study may not be accurate. First, the present approach is based on a uniform PS value throughout the cerebral cortex and cerebellum, which may not be true. In addition, the mathematical calculation

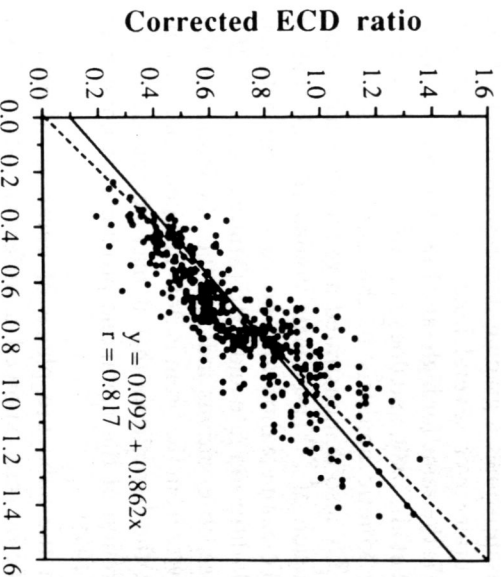
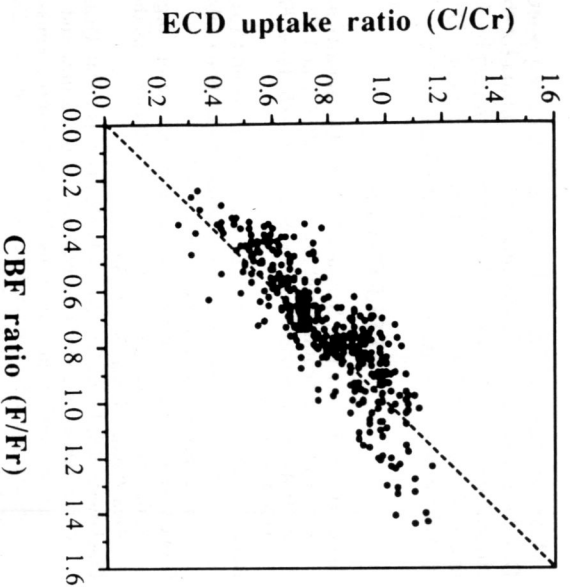


FIG. 5. Results of linearization on the relationship of the ^{99m}Tc -bicisate (ECD) uptake ratio and CBF ratio. The corrected ^{99m}Tc -bicisate uptake ratio demonstrated an excellent linear relationship with the CBF ratio ($y = 0.092 + 0.862x$, $r = 0.817$).

was based on the group average data and not on individual analysis. Similar calculation could be performed using the data in each individual subject, which would improve the accuracy of estimation. Another important point is that [^{15}O]water used as a reference tracer in this study also has limited extraction (Raichle et al., 1976). Considering the reported PS value of water of $\sim 130\text{--}140\text{ ml } 100\text{ ml}^{-1}\text{ min}^{-1}$, the actual PS value of $^{99\text{m}}\text{Tc}$ -bicisate should be $<71\text{ ml } 100\text{ ml}^{-1}\text{ min}^{-1}$. Lower spatial resolution in both transaxial plane and axial direction in the SPECT images also decreases the contrast between high- and low-flow regions, which might be partly responsible for the nonlinear relationship between CBF and SPECT count ratios. In spite of these limitations in accurate estimation of the PS value, the proposed linearization procedure can be used widely for correction of the clinical SPECT images because of its simplicity. For this purpose, it is necessary to validate this approach using another data set with wide flow range in a variety of physiological and pathological conditions.

Although a similar nonlinear relationship was observed with another Tc cerebral perfusion tracer for SPECT measurement, $^{99\text{m}}\text{Tc}$ -exametazime, the responsible kinetic behavior may be different from that of $^{99\text{m}}\text{Tc}$ -bicisate. The relatively poor image contrast between low-flow and normal-flow regions was mainly explained by the significant back-diffusion of lipophilic tracer from the brain immediately after the activity reached the brain (Andersen et al., 1988; Lassen et al., 1988; Murase et al., 1992a), and the nonlinearity correction was applied based on this back-diffusion model (Inugami et al., 1988; Yonekura et al., 1988). $^{99\text{m}}\text{Tc}$ -Bicisate shows a gradual decrease in activity from the brain over several hours, but the elimination rate is the same for high- and low-flow regions (Léveillé et al., 1989) and does not affect image contrast. The kinetic analysis in the clinical cases with SPECT also demonstrated a relatively small back-diffusion of $^{99\text{m}}\text{Tc}$ -bicisate compared with that of $^{99\text{m}}\text{Tc}$ -exametazime and no relationship between back-diffusion rate and CBF (Murase et al., 1992b). These observations indicate the elimination of the activity from the brain is flow independent and support the hypothesis that it may be related to the excretion of the metabolic products (Walovitch et al., 1991).

In the subacute phase of cerebral infarction, $^{99\text{m}}\text{Tc}$ -bicisate showed a different pattern from CBF. Compared with CBF, $^{99\text{m}}\text{Tc}$ -bicisate demonstrated markedly diminished uptake in the infarcted area where OEF and CMRO_2 showed a severe reduction of oxygen metabolism. The underlying

mechanism of this discrepancy is not clear at this moment. It may be related to the retention mechanism of $^{99\text{m}}\text{Tc}$ -bicisate in the normal brain structures and metabolism of the lipophilic complex to polar acid products (Walovitch et al., 1991). As this metabolic process is rapid, the distribution of the compound is proportional to CBF over a wide range (Orlandi et al., 1990). Therefore, diminished uptake of $^{99\text{m}}\text{Tc}$ -bicisate in subacute stroke may be due to the lack of oxygen and enzyme activity, resulting in the washout of unmetabolized tracer (Holman et al., 1989; Walovitch et al., 1991). The breakdown of the blood-brain barrier in stroke might also cause the leakage of activity from the brain (Moretti et al., 1990).

However, this characteristic of $^{99\text{m}}\text{Tc}$ -bicisate is of a great advantage for diagnosis of stroke. In contrast, $^{99\text{m}}\text{Tc}$ -exametazime shows a similar distribution pattern with CBF even in luxury perfusion or tumors, and in some cases it interferes with accurate diagnosis of the area and the extent of the infarction, although it can demonstrate the transient hyperemia in subacute stroke (Tsuchida et al., 1992). These findings suggest that the different characteristics of each cerebral perfusion tracer should be taken into consideration for clinical interpretation of brain perfusion SPECT images.

In conclusion, $^{99\text{m}}\text{Tc}$ -bicisate is a useful SPECT tracer for assessment of CBF, and the nonlinear relationship of flow and SPECT counts can be corrected based on the PS model. Although $^{99\text{m}}\text{Tc}$ -bicisate uptake is diminished compared with CBF in luxury perfusion, $^{99\text{m}}\text{Tc}$ -bicisate SPECT may be a valuable tool for the diagnosis of stroke including the subacute phase.

Acknowledgment: The authors gratefully acknowledge Drs. M. Ishikawa, H. Fukuyama, and N. Tamaki for their clinical support. This work was supported in part by Japanese Ministry of Education, Culture and Science Grant in Aid for Scientific Research (no. 03453282).

REFERENCES

- Andersen AR, Friberg HH, Schmidt JF (1988) Quantitative measurements of cerebral blood flow using SPECT and $^{99\text{m}}\text{Tc}$ -*l*-HM-PAO compared to xenon-133. *J Cereb Blood Flow Metab* 8:S69-S81
- Baron JC, Boussier MG, Comar D, Cattaigne P (1980) Crossed cerebellar diaschisis in human supratentorial brain infarction. *Trans Am Neurol Assoc* 105:459-461
- Crone C (1963) The permeability of capillaries in various organs as determined by use of the "indicator diffusion" method. *Acta Physiol Scand* 58:292-305
- Frackowiak RS, Lenzi GL, Jones T, Heather JD (1980) Quantitative measurement of regional cerebral blood flow and oxygen metabolism in man using ^{15}O and positron emission tomography: theory, procedure, and normal values. *J Comput Assist Tomogr* 4:727-736
- Kuhl DE, Barrio JR, Huang SC, Selin C, Ackerman RF, Lear JL, Wu JL, Lin TH, Phelps ME (1982) Quantifying local

- cerebral blood flow by *N*-isopropyl-*p*-[¹²³I]iodoamphetamine (IMP) tomography. *J Nucl Med* 23:196-203
- Kung HF, Guo YH, Yu CC, Billings J, Subramanian V, Calabrese J (1989) New brain imaging agents based on Tc-99m bis-aminoethanethiol (BAT) complexes: stereoisomers and biodistribution. *J Med Chem* 32:433-437
- Kung HF, Ohmomo Y, Kung M-P (1990) Current and future radiopharmaceuticals for brain imaging with single photon emission computed tomography. *Semin Nucl Med* 20:290-302
- Holman BL, Hellman RS, Goldsmith SJ, Mena IG, Léveillé J, Gherardi PG, Moretti J-L, Bischof-Delaloye, Hill TC, Rigo PM, Van Heertum RL, Ell PJ, Buell U, De Roo MC, Morgan RA (1989) Biodistribution, dosimetry, and clinical evaluation of technetium-99m ethyl cysteinate dimer in normal subjects and in patients with chronic cerebral infarction. *J Nucl Med* 30:1018-1024
- Inugami A, Kanno I, Uemura K, Shishido F, Murakami M, Tomura N, Fujita H, Higano A (1988) Linearization correction of ^{99m}Tc-labeled hexamethyl-propylene amine oxime (HMPAO) image in terms of regional CBF distribution: comparison to C¹⁵O₂ inhalation steady-state method measured by positron emission tomography. *J Cereb Blood Flow Metab* 8:S52-S60
- Lammertsma AA, Jones T (1983a) Correction for the presence of intravascular oxygen-15 in the steady-state technique for measuring regional oxygen extraction ratio in the brain: 1. Description of the method. *J Cereb Blood Flow Metab* 3:416-424
- Lammertsma AA, Wise RJS, Heather JD, Gibbs JM, Leenders KL, Frackowiak RSJ, Rhodes CG, Jones T (1983b) Correction for the presence of intravascular oxygen-15 in the steady-state technique for measuring regional oxygen extraction ratio in the brain: 2. Results in normal subjects and brain tumour and stroke patients. *J Cereb Blood Flow Metab* 3:425-431
- Lassen NA (1985) Cerebral blood flow tomography with xenon-133. *Semin Nucl Med* 15:347-356
- Lassen NA, Anderson AR, Friberg L, Paulson OB (1988) The retention of [^{99m}Tc]-*d,l*-HM-PAO in the human brain after intracarotid bolus injection: a kinetic analysis. *J Cereb Blood Flow Metab* 8:S13-S22
- Léveillé J, Demonceau G, De Roo M, Rigo P, Taillefer R, Morgan RA, Kupranick D, Walovitch RC (1989) Characterization of technetium-99m-*L,L*-ECD for brain perfusion imaging, part 2: biodistribution and brain imaging in humans. *J Nucl Med* 30:1902-1910
- Léveillé J, Demonceau G, Walovitch RC (1992) Intersubject comparison between technetium-99m-ECD and technetium-99m-HMPAO in healthy human subjects. *J Nucl Med* 33:480-484
- Moretti JL, Defer G, Cinotti L, Cesaro P, Degos J-D, Vigneron N, Ducassou D, Holman L (1990) "Luxury perfusion" with ^{99m}Tc-HMPAO and ¹²³I-IMP SPECT imaging during the subacute phase of stroke. *Eur J Nucl Med* 16:17-22
- Murase K, Tanada S, Fujita H, Sakai S, Hamamoto K (1992a) Kinetic behavior of technetium-99m-HM-PAO in the human brain and quantification of cerebral blood flow using dynamic SPECT. *J Nucl Med* 33:135-143
- Murase K, Tanada S, Inoue T, Sugawara Y, Kimura Y, Sakai S, Hamamoto K (1992b) Kinetic behavior of Tc-99m ECD in the human brain using compartment analysis and dynamic SPECT: comparison with Tc-99m HMPAO. *J Nucl Med* 33:909
- Neirinckx R, Canning L, Piper I, Nowotnik DP, Pickett RD, Holmes RA, Volkert WA, Forster AM, Weisner PS, Marriot JA, Chaplin SB (1987) Technetium-99m-*d,l*-HM-PAO: a new radiopharmaceutical for SPECT imaging of regional cerebral blood perfusion. *J Nucl Med* 28:191-202
- Orlandi C, Crane PD, Platts SH, Walovitch RC (1990) Regional cerebral blood flow and distribution of [^{99m}Tc]ethyl cysteinate dimer in nonhuman primates. *Stroke* 21:1059-1063
- Raichle ME, Eichling JO, Straatmann MG, Welch MJ, Larson KB, Ter-Pogossian MM (1976) Blood-brain barrier permeability of ¹¹C-labeled alcohols and ¹⁵O-labeled water. *Am J Physiol* 230:543-552
- Sadato N, Yonekura Y, Senda M, Iwasaki Y, Matoba N, Tamaki N, Sasayama S, Magata Y, Konishi J (1993) Positron emission tomography and the autoradiographic method with continuous inhalation of ¹⁵O gas: theoretical analysis and comparison with conventional steady-state method. *J Nucl Med* 34:1672-1680
- Stokely EM, Sveinsdottir E, Lassen NA, Rommer P (1980) A single photon dynamic computer-assisted tomograph (DCAT) for imaging brain function in multiple cross-sections. *J Comput Assist Tomogr* 4:230-240
- Tsuchida T, Yonekura Y, Sadato N, Iwasaki Y, Tamaki N, Konishi J, Fujita T, Matoba N, Nishizawa S, Magata Y (1992) Brain perfusion SPECT with [^{99m}Tc]-*L,L*-ethyl cysteinate dimer (ECD) in comparison with regional cerebral blood flow measured by PET: underestimation in the high flow range. *J Nucl Med* 33:966-967
- Vallabhajosula S, Zimmerman RE, Picard M, Stritzke P, Mena I, Hellman RS, Tikofsky RS, Stabin MG, Morgan RA, Goldsmith SJ (1989) Technetium-99m ECD: a new brain imaging agent: in vivo kinetics and biodistribution studies in normal human subjects. *J Nucl Med* 30:599-604
- Walovitch RC, Hill TC, Garrity ST, Cheesman EH, Burgess BA, O'Leary DH, Watson AD, Ganey MV, Morgan RA, Williams SJ (1989) Characterization of technetium-99m-*L,L*-ECD for brain perfusion imaging, part 1: pharmacology of technetium-99m ECD in nonhuman primates. *J Nucl Med* 30:1892-1901
- Walovitch RC, Franceschi M, Picard M, Cheesman EH, Hall KM, Makuch J, Watson MW, Zimmerman RE, Watson AD, Ganey MV, Williams SJ, Holman BL (1991) Metabolism of ^{99m}Tc-*L,L*-ethyl cysteinate dimer in healthy volunteers. *Neuropharmacology* 30:283-292
- Winchell HS, Baldwin RM, Lin TH (1980a) Development of I-123 labeled amines for brain studies: localization of I-123 iodophenylalkylamines in rat brain. *J Nucl Med* 21:940-946
- Winchell HS, Horst WD, Braun L, Oldendorf WH, Hattner R, Parker H (1980b) *N*-Isopropyl-[¹²³I]*p*-iodoamphetamine: single-pass brain uptake and washout; binding to brain synaptosomes; and localization in dog and monkey brain. *J Nucl Med* 21:947-952
- Yamauchi H, Fukuyama H, Yamaguchi S, Doi T, Ogawa M, Ouchi Y, Kimura J, Sadato N, Yonekura Y, Tamaki N, Konishi J (1992) Crossed cerebellar hypoperfusion in unilateral major cerebral artery occlusive disorders. *J Nucl Med* 33:1632-1636
- Yonekura Y, Nishizawa S, Mukai T, Fujita T, Fukuyama H, Ishikawa M, Kikuchi H, Konishi J, Andersen AR, Lassen NA (1988) SPECT with ^{99m}Tc-*d,l*-hexamethylpropylene amine oxime (HMPAO) compared with regional cerebral blood flow measured by PET: effects of linearization. *J Cereb Blood Flow Metab* 8:S82-S89
- Yonekura Y, Fujita T, Nishizawa S, Mukai T, Koide H, Yamamoto K, Tamaki N, Konishi J, Hirose Y (1989) Multidetector SPECT scanner for brain and body: system performance and applications. *J Comput Assist Tomogr* 13:732-740